Calibration of the KIT Test Setup for the Cooling Tests of a Gyrotron Cavity Full-size Mock-up Equipped with Mini-channels

Sebastian Stanculovic[a], Rosa Difonzo[b], Andrea Allio[b], Konstantinos A. Avramidis[a], Philip Brücker[a], Gerd Gantenbein[a], Stefan Illy[a], John Jelonnek[a,c], Parth C. Kalaria[a], Moritz Misko[a], Tomasz Rzesnicki[a] and Laura Savoldi[b]

[a]*Institute for Pulsed Power and Microwave Technology, Karlsruhe Institute of Technology (KIT), Karlsruhe, Germany,*

[b]*Dipartimento Energia "Galileo Ferraris", Politecnico di Torino, Torino, Italy*

[c]*Institute of Radiofrequency Engineering and Electronics (IHE), Karlsruhe Institute of Technology (KIT), Karlsruhe, Germany,*

Abstract: In high-power fusion gyrotrons, the maximum heat-load on the wall of the interaction section is in the order of 2 kW/cm^2, which is the major limiting technological factor for output power and pulse-length of the tube. The ongoing gyrotron development demands a very effective cavity cooling system for optimum gyrotron operation. In this work, the experimental investigation of a mini-channel cavity cooling using a mock-up test set-up is described. The mock-up test set-up will be used to experimentally validate the predictive simulation results and verify the mini-channel cooling performance. It is crucial for validation of the mini-channel cooling properties to determine the amount of the heat load introduced in the cavity wall by an induction heater. In order to estimate that heat load, full 3D electromagnetic simulations have been performed using the CST Studio Suite® software. A suitable calibration factor for the load deposited in the mock-up inner wall is identified after numerical investigation by a 3D thermal model. Calorimetry measurements are performed and the experimental results are compared with the simulation results obtained with a 3D thermal-hydraulic model, using the commercial software STAR-CCM+. When the calibration factor is applied, the experimental calorimetry is well reproduced by the simulations.

Keywords: gyrotron, mini-channel cavity cooling, experimental validation, multi-physics simulations, nuclear fusion.

1. Introduction

For Electron Cyclotron Resonance Heating and Current Drive (ECRH& CD) applications in thermonuclear fusion experiments the high-power (~ 1 – 2 MW) gyrotrons are the prominent RF sources [1]. For ITER, a 2 MW, 170 GHz coaxial cavity gyrotron and a 1 MW, 170 GHz hollow cavity gyrotron have been developed by the European GYrotron Consortium (EGYC) in cooperation with the industrial partner Thales Electron Devices (TED) [2]. Nominal ohmic heat-load of the cavity in these gyrotrons is high (~ 2 kW/cm^2). Integral of the power loss in the cavity is ~60kW. A figure of the calculated heat distribution on the outer cavity wall of a 2 MW coaxial gyrotron is shown in [3], together with the geometry of the coaxial cavity. This cavity-wall heating in long-pulse gyrotron operation causes a thermal deformation which leads to a downshift of the gyrotron operating frequency [4]. Hence, an effective cavity cooling system is a prerequisite to maintain the cavity temperature within material strength limits (e.g. 250°C for the Glidcop).

A simple annular gap cavity cooling system is used in a modular and demountable 170 GHz, 2 MW short-pulse coaxial-cavity gyrotron [5]. It should be mentioned here that an annular gap cooling is not used in the industrial CW gyrotrons. The cooling performance of the existing annular gap cavity cooling system is evaluated in [6] using multi-physics iterative simulations. Simulation results suggest safe gyrotron operation up to a pulse length of 150 ms [3], within the temperature limit of 250°C. With an increasing the pulse length up to 500 ms, the steady-state temperature of the cavity wall also increases up to 360°C. Thus, an advanced cooling system is required to increase the pulse-length and to improve the frequency stability. A mini-channels cavity cooling system and its capability are studied for the 170 GHz, 1 MW hollow-cavity EU gyrotron [7].

The mini-channel cooling approach has been investigated at the Karlsruhe Institute of Technology (KIT) for an effective resonator cooling. Its thermal performances for resonator cooling of a 2 MW, 170 GHz coaxial gyrotron have been numerically investigated using the ANSYS Fluent® software [8], as well as using the MUlti-physiCs tool for the integrated simulation of the CAvity (MUCCA), in collaboration between Politecnico di Torino and KIT. Cooling of the inner conductor of the coaxial cavity in the 2 MW, 170 GHz coaxial gyrotron is not an issue [9] and in the present paper only the cooling of the cavity wall is discussed.

A test mock-up consisting of 40 mini-channels, with geometry and materials that correspond to the real gyrotron cavity, is developed at KIT and integrated into the experimental set-up. The inner diameter of the mock-up is 59 mm, which is also the diameter of the 170 GHz ITER gyrotron cavity. Inner part of the mock-up is

fabricated from Glidcop AL-15® material, and the outer jacket is from stainless steel. Nominal distance of the cooling channels to the inner cavity wall surface of the mock-up is 3.95 mm.

Proposed mini channel cooling has two inlets and two outlets, that are rotated by 180°, in order to homogenize the cooling [8]. Mini-channels have semicircular cross section with radius of 1.4 mm and length of 45 mm in the flow direction.

For an evaluation of the cooling performances 16 thermocouples, pressure sensors and a flow meter are installed into experimental installation. The induction heater (MINAC 6®, EFD Induction) induces, at the power level of 3000 W, the thermal loads up to ~1.2 MW/m^2 on the cavity inner wall. Acquisition sub-system is implemented in the cavity cooling test system for visualization and recording of the measured values.

In the first experiments with only heating, without the flow of the cooling water, the temperature curves at different points in the mock-up cavity wall have been recorded. In calorimetry tests, by measuring the temperatures on inlets and outlets, the integral of the induced thermal load is calculated.

It is crucial for validation of the mini-channel cooling properties to determine the amount of the introduced thermal losses in the cavity wall with the induction heater. In order to estimate the induced thermal losses, full 3D electromagnetic (EM) simulations have been performed with the CST Studio Suite®. A calibration factor for the EM model results has been then computed, based on the first set of experimental data, by comparison with the results of extensive pure thermal 3D simulations.

Results of the calorimetry tests have been used to validate the computed calibration factor, reproducing the experimental results by mean of a 3D fully thermal-hydraulic model, implemented in the MUCCA tool.

2. Experiments

2.1 Experimental set-up

The experimental set-up consists of a mock-up, 20 temperature sensors, two pressure sensors and a flow meter. As a cooling liquid is used the demineralized subcooled water, which is pumped through the mock-up in a closed loop system. Block schematic of the set-up is illustrated in Fig. 1.

The 16 thermocouples (TC) type K with 1 mm diameter are positioned in the cavity wall at 4 different distances from the inner wall surface: 1.2 mm, 2 mm, 5 mm and 6.5 mm. In the direction parallel to the mock-up axis, eight of these thermocouples are positioned in the center plane ($z = 0$) and four TCs are placed in the planes $z = 15$ mm and $z = -15$ mm, respectively.

Additionally to 16 thermocouples, four thermal sensors PT100 (resistivity thermometers) are integrated in the inlets and outlets, in order to perform the calorimetry measurements.

Pressure sensors measure the pressures at the upper inlet and outlet, giving the pressure difference between them. One flow meter is positioned before the splitting of the water line into the two inlets and measures the total water flow.

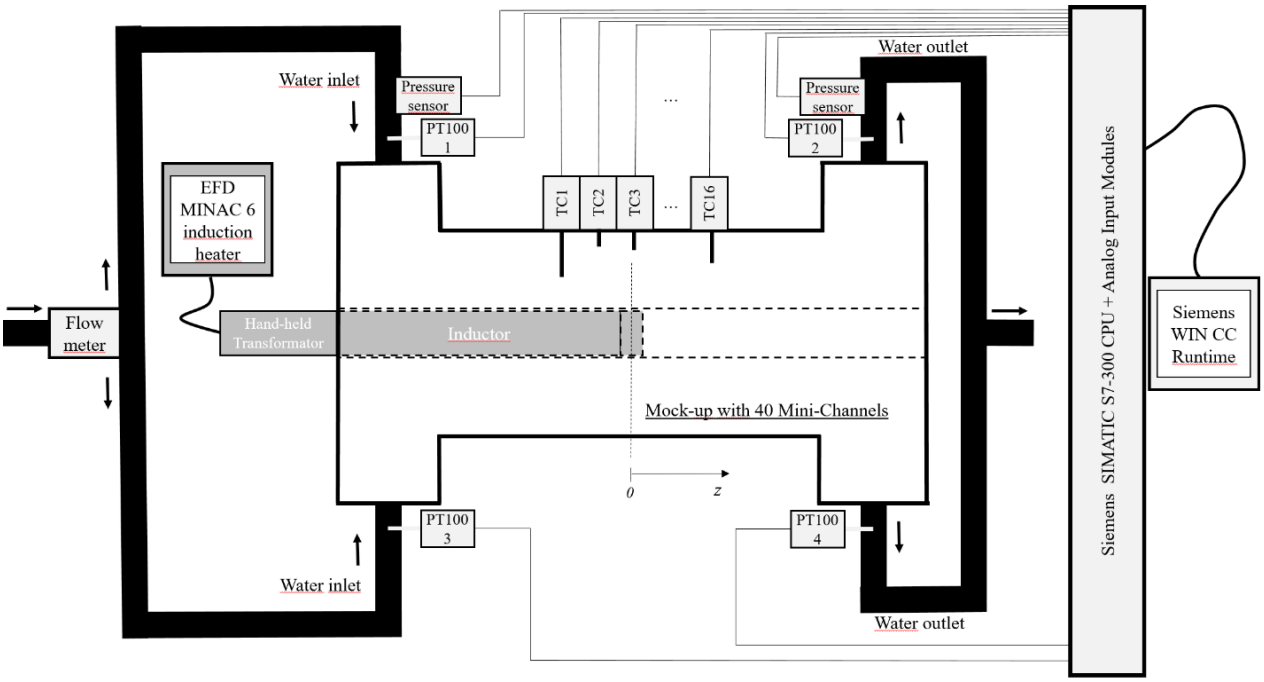

Fig. 1. Block diagram of the experimental set-up: mini-channel cooling mockup, thermocouples (TC1… TC16), PT100 thermometers (PT100 1 – PT100 4), pressure sensors, flow meter, MINAC6 inductor heater with hand-held transformer and the inductor head, as well as SIMATIC S7-300® hardware and a computer with WIN CC® software.

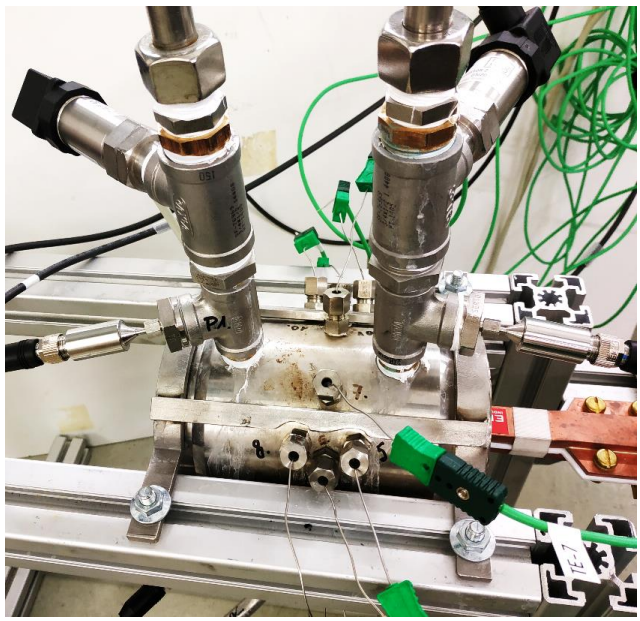

Fig. 2. Complete experimental set-up: mini-channel cooling mockup, thermal sensors, pressure sensors and the inductor heating coil.

The experimental installation is depicted in Fig. 2.

MINAC 6® induction heater of the EFD Company provides the maximal heating power of 10 kW. The geometry of the inductor head is chosen to fit into the presented mini-channels mock-up, to improve the efficiency of the induction heater and to fairly simulate the heat load spatial distribution in the coaxial gyrotron cavity. Outer diameter of the inductor head, with a one loop copper coil, is 57 mm (Fig. 3), assuring a safe insertion of the inductor head into the mock-up with 59 mm inner diameter and reducing the possibility of hazardous touching of the inductor head and the mock-up inner wall. Additionally, the air gap of only 1 mm between the coil head and the inner mock-up wall maximizes the efficiency of the heating. The axial length of the cooper stripe of the coil loop is set to 8 mm. This length provides a localized heating in the section of the inner mock-up wall with the length of ~ 10 mm, which approximately corresponds to the width of the cavity section with the peak thermal load in the 2 MW coaxial gyrotron [3]. Further, the total length of the induction coil is chosen to enable a comfortable positioning of the coil head in the middle cross section of the mock-up (z = 0), where eight of the thermocouples are inserted.

Impedance matching between the hand-held transformer and the heating inductor coil is unknown. The exact value of the AC current flowing in the inductor during the heating is also not determined, because a measurement of this current is very demanding and difficult. Complexity of the current measurement is due to the large dimension of the inductor coil, very high currents (50 – 100 A) and high working frequencies (20 kHz – 50 kHz). The level of AC current has been firstly estimated using a practical formula provided by company of EFD induction in a private communication. This estimation has been evaluated and corrected in thermal simulations and validated in calorimetry calibrations.

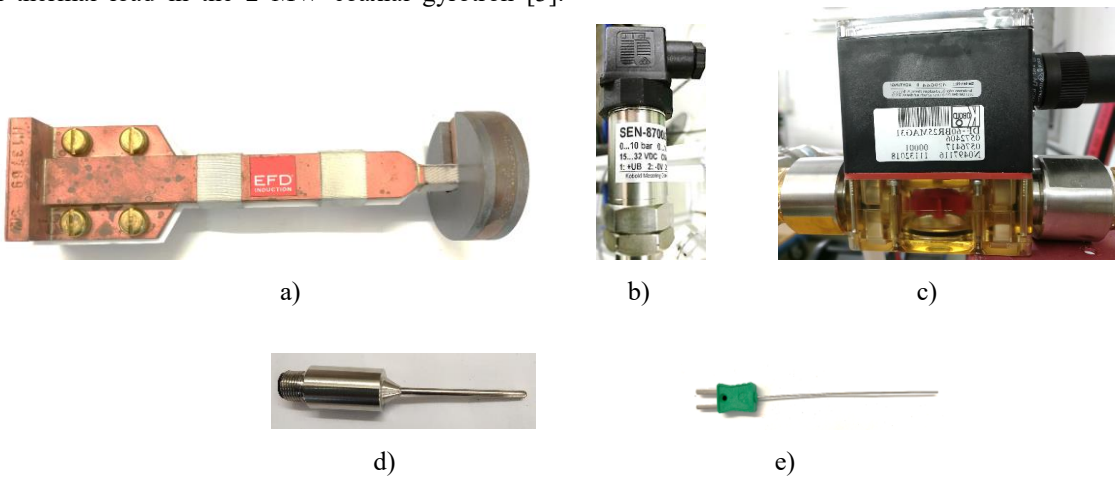

a) b) c)

d) e)

Fig. 3. Elements of experimental hardware: a) Inductor heating coil, b) pressure sensor, c) flow meter, d) PT100 resistivity thermometer and e) thermocouple type K.

Described induction heater provides a well-defined localized, controllable and reliable heating. It satisfies requirements of experiments for a direct comparison of mini-channel heating to other standard cooling techniques, such as the Raschig rings cooling. It is also advantageous for experimental validation of 3D thermal-hydraulic numerical simulations. Disadvantage of the chosen induction heater is its limited power of 10 kW. This power level cannot provide the thermal load of 2 kW/cm^2, which is expected in the cavity of the 2 MW gyrotron. This trade-off can be compensated by using advanced 3D thermal-hydraulic simulations, that are experimentally calibrated and validated, for investigating the mini-channel cooling also for the very high thermal fluxes up to 2 kW/cm^2.

The acquisition system consists of the Siemens Simatic S7-300® CPU and analog input modules for a signal processing and of the Siemens software WinCC Runtime® for visualization and recording of the measured data. The test system has the acquisition frequency of 1 Hz.

2.2 Heating experiments

In first heating tests the temperatures in the cavity wall have been measured in order to determine the effectiveness of the induction heater EFD MINAC 6®. These measurements are performed without the flow of the water coolant and the temperatures of 16 thermocouples are recorded for following set powers at the inductor heater: 1800 W, 2400 W and 3000 W, for 10 min in first case and for 5 min in the last two cases. Due to the impedance mismatching between the inductor coil and the hand-held transformer, the applied power level in experiments was restricted up to 3300 W.

2.2.1 Calorimetry measurements

In calorimetry tests the temperatures at the inlets and the outlets are determined for different water flows and heating powers. Total flows of 10 l/min and 20 l/min are considered, as well as power levels of 1800 W, 2400 W and 3000 W.

3. Simulations

3.1 Electromagnetic simulations

In order to estimate the inserted thermal losses into the cavity wall a 3D model is constructed using the CST Studio Suite. The calculations have been performed in a frequency domain solver at the AC frequency of 25 kHz, which corresponds to the work frequency in the experiments. Simulation model of the induction heater has the same geometry as the real inductor coil. The simulation port is positioned at the heating coil. Open boundary conditions have been defined in the EM simulations, corresponding to the laboratory environment where the mock-up is installed, see Figure 2.

Electrical conductivity of the GLIDCOP AL-15® material is set to the value of 54 MS/m, which is a DC electrical conductivity at room temperature [10].

Radio frequency (RF) power that excites the simulation model is firstly set to the nominal heating power levels from the heating experiments. Surface losses in the lossy metallic parts are calculated and provided as input heat fluxes to the thermal simulations.

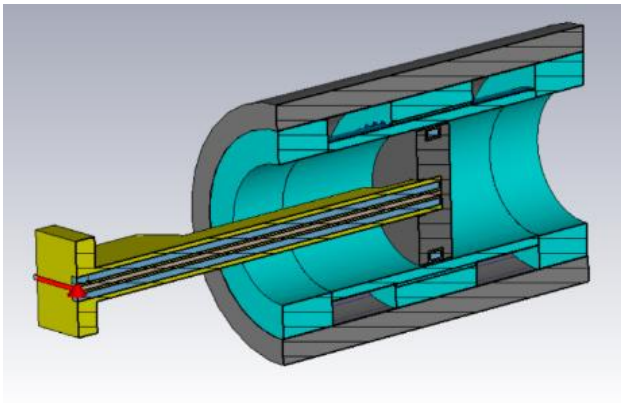

Fig. 4. Model for EM simulations: mini-channel mock-up with inserted inductor heater head

3.2 Thermal model

The uncertainties hidden in the EM model calls for a calibration of the heating power, for which dedicated test campaign of the mock-up without active cooling has been performed, see above. A pure thermal transient 3D model for the cavity mock-up has been developed using the commercial software STAR-CCM+ [11], based on the geometry shown in Figure 5, where sample is assumed to be "floating" (no thermal bridges to the supports), and the holes drilled to insert the thermocouples (TC) have been ignored.

An implicit unsteady model with time step = 0.1 s and 15 inner iterations has been proved to give robust results, on a mesh with 1.6 M Cells, providing grid-independent results. A polyhedral mesh has been used, refining the zone of the cavity near the high heat load, where the thermocouples are located. Temperature-dependent material properties have been used in the simulations for both stainless-steel (SS) and Glidcop. Thermal contact resistances have been conservatively imposed on the solid interfaces, equal to 1.0E-04 m^{2}K/W for the Glidcop/Glidcop interface and 5.0E-04 m^{2}K/W for the SS/SS interface, but the impact of this parameter has been checked a posteriori to be negligible on the computed results.

The heat load to the cavity wall computed with the EM model for different inductor power levels (600 W - 1800 W) has been applied to the inner wall of

the cavity (red surface in Figure 5) while all the other walls have been considered adiabatic. The initial temperature (T_0) for the entire mock-up has been set equal to the measured ambient temperature (T_{amb}) of 24.3°C. All the simulations have been run up to 600 s.

3.2.1 Inductive power calibration

In the evaluation of the computed results, the temperature at the TC has been computed as a surface average of a 1-mm sphere around the nominal location of the TC, assuming a perfect contact between the TC head and the Glidcop. The comparison between the computed and experimental evolution of the temperature increase at the TC locations shows, independently on the power level, a large underestimation in the simulations, see Figure 6.

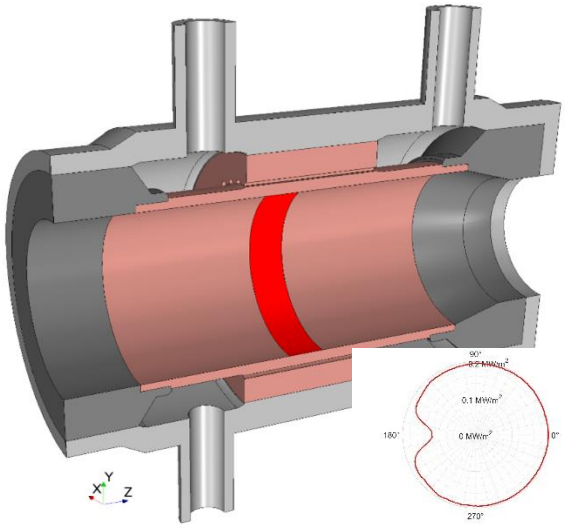

Fig. 5. Section of the geometry used for the mock-up thermal model. The grey solids refer to stainless-steel, the pink parts to Glidcop. In the insert: azimuthal distribution of the load on the cavity surface, as from the EM simulations with 1800 W of inductor power

A calibration procedure has been carried out to evaluate the correction factor to be applied to the EM results from the ratio between the experimental and computed traces. For each TC trace we first evaluate $y_i(t)$, which is the instantaneous ratio of the experimental temperature increase to the computed one for the i-th TC, as in Eq. (3). Note that the temperature increases are all evaluated with respect to the ambient temperature.

$$y_i(t) = \frac{dT_{exp}(t)}{dT_{comp}(t)} \quad (3)$$

The values of $y_i(t)$ are then averaged for the whole set of 16 thermocouples, returning $y_{gl}(t)$ as from Eq. (4).

$$y_{gl}(t) = \frac{\sum_{i=1}^{16} y_i(t)}{16} \quad (4)$$

The correction factor α_{HL} has been computed at each heat load (HL), obtained averaging $y_{gl}(t)$ on the time, starting from the time t_{start} as shown in Eq. (5).

$$\alpha_{HL} = \frac{\sum_{t=t_{start}}^{600\ s} y_{gl}(t_j)}{(600\ s - t_{start})} \quad (6)$$

In Eq. (6), t_{start} has been parametrically increased to find values of α_{HL} independent on its arbitrary choice, see Figure 7. The asymptotic values of α_{HL} computed for the three values of nominal power are the same within the error bar and the final calibration factor α can be computed by averaging resulting in Eq. (7) with its estimated accuracy.

$$\alpha = 2.04 \pm 0.04 \quad (7)$$

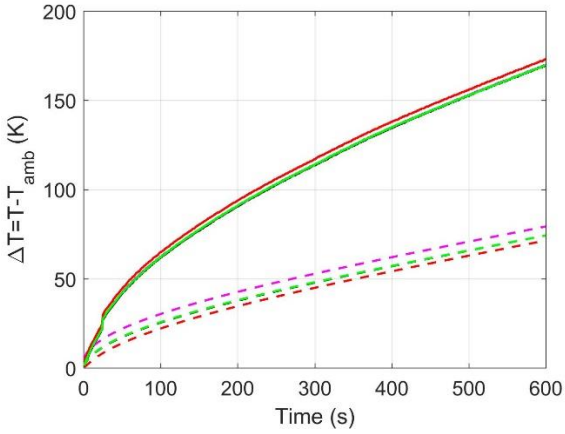

Fig. 6. Measured temperature evolution at TCs 9, 10, 11 and 12 (solid lines) with the corresponding computed values (dashed curves), at the inductor power level of 1800 W.

3.3 Thermal-hydraulic model

A 3D steady-state conjugate thermal-hydraulic model has been then developed, again using the commercial software STAR-CCM+ [11]. Since the mock-up is cooled by subcooled water entering the cooling region by two different inlets in parallel, the model for the thermal-hydraulic simulations also includes T-junctions upstream and downstream of the mock-up (Figure 8) to allow the balanced flow computed in the two branches.

The well-established κ–ω SST turbulence model with all y^+ wall treatment is adopted in the simulations since it is able to capture the flow detachment downstream of the mini-channels region. Calorimetry test have been performed at 0.17 and 0.34 kg/s of total mass flow rate. In the first case, the flow in the mini-channels is in transition flow regime, therefore a gamma-transition model has been adopted.

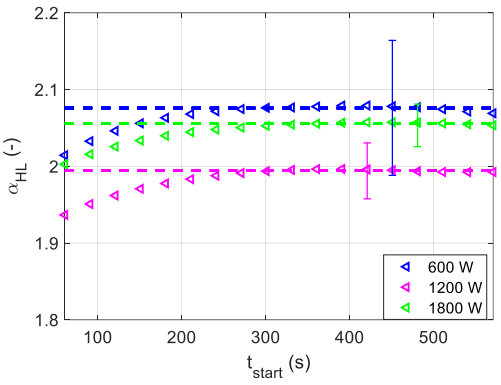

Fig. 7. Calibration factor computed as a function of the arbitrary choice of t_{start} (symbols) for the different HL values. The asymptotic values (dashed lines) used to evaluate the mean calibration factor α are also reported.

The mesh built in the fluid domain account for 12M cells, with a core-flow base size of 0.15 mm. The thickness of the first wall prism layer has been defined in order to obtain a $y^+ \sim 1$.

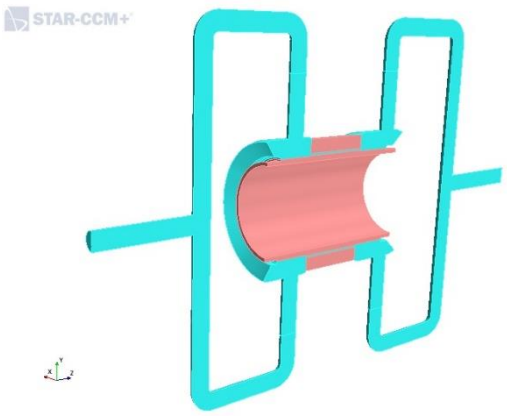

Fig. 8. Sketch of the reference geometry for the full 3D thermal-hydraulic simulations, including also the water domain (in light blue). Half of the computational domain is shown.

For the solid domain, including the cavity and the water stopper, a 3D, steady-state thermal model has been adopted. As in the previous model, the calibrated heat load has been imposed on the inner surface of the cavity while all the other walls have been considered adiabatic.

The conjugate heat transfer problem is solved using a segregated approach for the energy equation. The thermal driver is obtained from the EM model, corrected by the factor α computed in the calibration exercise (see Eq. (7)). An inlet water mass flow of 0.17 (and 0.34) kg/s at 23°C is used as inlet condition for the fluid domain, and a pressure of 1 bar is imposed at the outlet.

4. Calorimetry results

The measurements from the preliminary experimental campaign, devoted to the calorimetric assessment of the heat load on the cavity have been carefully analyzed to check the calibrated value of the heat load in the simulations. The calibration tests were performed at different flow rates, varying the inductor power and, also, swapping the flow direction.

A check of the robustness of the recipe adopted for the assessment of the heat load by the inductive heater is first carried out at a global level, cross-checking the calibrated heat load used in the simulations with the heat load computed from the experimental calorimetry, see Figure 9, following Eq. (8).

$$Q^{exp} = \dot{m}^{exp} \times c_p \times \left(T_{out}^{exp} - T_{in}^{exp}\right) \quad (8)$$

where Q^{exp} is the heat load calculated from the experimental results, $\dot{m}^{exp}$ is the total measured water mass flow rate in the cavity, c_p its specific heat, T_{out}^{exp} and T_{in}^{exp} are the outlet and inlet water temperatures, averaged on the two inlets and outlets of the mock-up. The calorimetry check is reported in Figure 10, showing that the calibrated values fall within the uncertainty range of the experimental points at all the power levels.

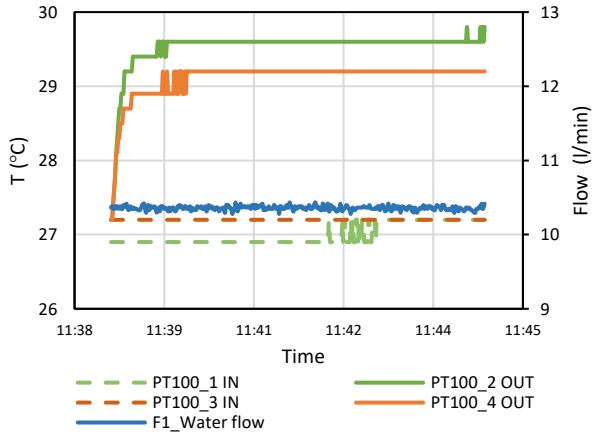

Fig. 9. Typical measured temperature curves after 6 min heating with 3000 W.

The values of the temperature increase at the outlet of each cooling branch of the mock-up, with respect to their respective inlet values, are collected in Figure 11. All measurements, performed by Pt-100 sensors, have an accuracy of 0.2 K. As expected, the temperature increase is larger when the coolant flow rate is smaller. For all the tests performed with the first flow direction (from left to right in Figure 4), the temperature increase of the top cooling path is consistently higher than that of the bottom path. Note that an unbalance of the flow distribution

between the two cooling paths has been ruled out by dedicated flow measurements performed as check on the two branches separately. The fact that almost no temperature increase unbalance is visible, when the flow direction is reversed, points at the possible presence of a thermal bridge or small heat sink between the heated region and the outlet (in the initial flow direction).

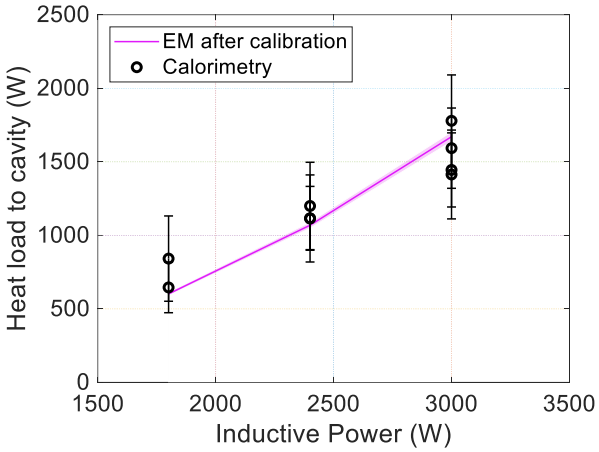

Fig. 10. Calorimetry check: heat load values from the EM model, after the calibration correction (solid line), compared to the measured values from calorimetry (open circles), with the respective uncertainty range.

In Figure 11, the simulated values corresponding to a sub-set of the test conditions are also reported (the same value is always computed for both cooling paths), and it is shown that they are in good agreement with the measured values, thus confirming the soundness of the inductive heat load calibration.

5. Conclusion and outlook

Heating experiments using a mock-up of a 2 MW gyrotron cavity with mini-channel cooling have been performed. In a first step, for calibration measurements, no cooling water was flowing through the channels. Thermal loads on the inner cavity wall are estimated by an EM model. This estimation has been calibrated by comparing experimental temperatures and values computed with pure thermal 3D simulations, identifying a suitable calibration factor for the heat load from the EM model.

Calorimetry tests with different flow rates and inductor power levels have been performed, and the measured results well match, in terms of global power to the coolant and coolant temperature at the outlet of the mock-up, with those computed using the heat load in 3D thermal-hydraulic simulations. The evaluation of the calibrated heat load deposited by the inductive heater can be now considered robust, and in perspective it can be used for the interpretation of the experimental results by means of the MUCCA tool.

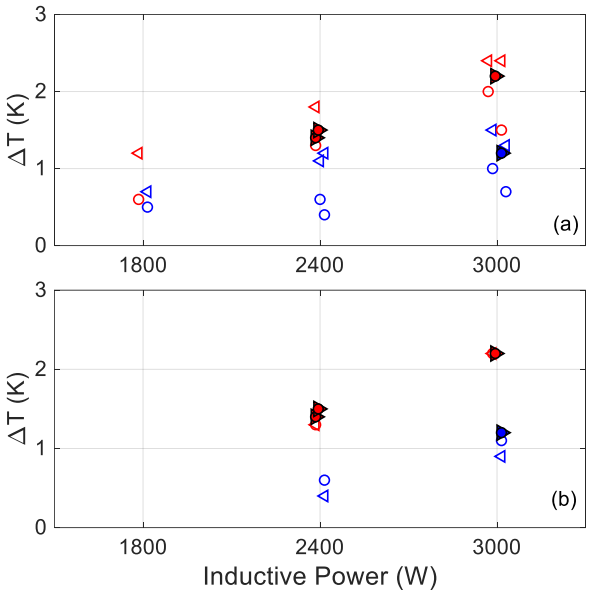

Fig. 11. Measured and computed temperature increase across the mock-up, for direct flow (a) and reverse flow (b) conditions, for tests with a total flow rate of 10 l/min (red symbols) and 20 l/min (blue symbols). Solid symbols (with black outline) = computed values, open symbols = measured values. The circles refer to the bottom cooling path, while the triangles refer to the top cooling path.

Preliminary results of the experimental investigations proved that the mini-channels are efficient for cooling. In order to evaluate the mini-channel cooling concept also for the very high power CW gyrotrons, thermal-hydraulic simulations with experimentally validated model and the accordingly up-scaled heat fluxes are planned to be performed.

Experiments for a direct comparison of mini-channel cooling to the cooling with Raschig rings will be conducted, using the mock-ups with equal geometries, that correspond to the cavity of 2 MW coaxial gyrotron, and under equivalent test conditions. The Raschig rings cooling is one of the standard industrial technologies for present high power gyrotrons. A direct experimental comparison between the two cooling techniques will indicate the appropriateness of the mini-channel cooling approach for the next generation of 2 MW CW gyrotrons.

Acknowledgments

We acknowledge the use of the computational resources provided by hpc@polito, which is a project of Academic Computing within the

Department of Control and Computer Engineering at the Politecnico di Torino (http://hpc.polito.it).

This work has been carried out within the framework of the EUROfusion Consortium and has received funding from the Euratom research and training programme 2014-2018 and 2019-2020 under grant agreement No 633053. The views and opinions expressed herein do not necessarily reflect those of the European Commission.

References

[1] M. Thumm, "Recent advances in the worldwide fusion gyrotron development," *IEEE Trans. Plasma Sci.*, vol. 42, no. 3, pp. 590–599, 2014, doi: 10.1109/TPS.2013.2284026.

[2] J. Jelonnek, *et al.*, "2018 Status on KIT Gyrotron Activities", EPJ Web Conferences, vol. 187, no. 01009, 2018, available online, doi: 10.1051/epjconf/201818701009.

[3] A. Bertinetti, *et al.*, "Analysis of an actively-cooled coaxial cavity in a 170 GHz 2 MW gyrotron using the multi-physics computational tool MUCCA", Fusion Engineering and Design, Nov. 2018, in press, available online, doi: 10.1016/j.fusengdes.2018.11.033.

[4] K. A. Avramidis, *et al.*, "Numerical Studies on the Influence of Cavity Thermal Expansion on the Performance of a High-Power Gyrotron," *IEEE Transactions on Electron Devices*, vol. 65, no. 6, pp. 2308-2315, 2018, doi: 10.1109/TED.2017.2782365.

[5] S. Ruess, *et al*., "KIT Coaxial Gyrotron Development: From ITER towards DEMO", International Journal of Microwave and Wireless Technologies, vol. 10, no. 5-6, pp. 547-555, 2017, available online, doi: 10.1017/S1759078718000144.

[6] L. Savoldi, *et al*, "Assessment and optimization of the cavity thermal performance for the European Continuous Wave gyrotrons," presented in 27th IAEA Fusion Energy Conference, Gandhinagar, India, 2018.

[7] A. Bertinetti, *et al.*, "Multi-physics analysis of a 1 MW gyrotron cavity cooled by mini-channels", Fusion Engineering and Design, vol. 123, pp. 313-316, May 2017, available online, doi: 10.1016/j.fusengdes. 2017.05.016.

[8] P. T. Brücker, "Development of an Innovative Water Cooling System for highly loaded Gyrotron Resonators", Bachelor Thesis, Karlsruhe Institute of Technology, 2018.

[9] P. C. Kalaria, *et al*., "Multi-physics modeling of insert cooling system for 170 GHz, 2 MW long-pulse coaxial-cavity gyrotron", IEEE Tran. On Electron Devices, 66, 4008-4015, 2019, available online, doi: 10.1109/TED.2019.2928222.

[10] GLIDCOP AL-15® Datasheet, https://www.hoganas.com/globalassets/download-media/sharepoint/brochures-and-datasheets---all-documents/glidcop_al-15.pdf. 2020.03.05.

[11] Star-CCM+ User's Guide v 15.02; Siemens PLM Software Inc.: Plano, TX, USA, 2020.